

Impact of La on Structural, Morphological and Magnetic Properties of NiCoFe₂O₄ Nano Ferrites

P. K. Nagpure^a, A. K. Nandanwar^b, V. M. Nanoti^c and K. G. Rewatkar^b

^a Department of Physics, D.B. Science College, Gondia-441614, Maharashtra, India.

^b Department of Physics, Dr. Ambedkar College, Deekshabhoomi Nagpur-440010, Maharashtra, India.

^c Department of Physics, PIET, Nagpur-440019, Maharashtra, India.

Doi: <https://doi.org/10.47011/15.1.3>

Received on: 01/08/2020;

Accepted on: 16/12/2020

Abstract: Ni_{0.2}Co_{0.8}Fe_{2-x}La_xO₄ (x = 0.02, 0.06, 0.10) nano ferrites have been synthesized by Sol-gel auto combustion method using urea as a fuel. The sample calcinations have been performed at 800 °C for 4 hours. The synthesized samples were subjected to study X-ray diffraction spectroscopy (XRD) for structural investigations. All the samples were found to constitute Face Centered Cubic (FCC) spinel structure belonging to the Fd3m space group. The XRD results show the single cubical phase formation in the heated samples. Energy-dispersive X-ray spectra confirmed the presence of Ni, Co, La Fe and O elements with no existence of any impurity. The average crystallite size was decreased by varying the concentration of La from 10 to 8 nm. The Field Emission Gun Scanning Electron microscopy (FEG-SEM) and Field Emission Gun transmission electron microscopy (FEG-TEM) have given the morphological study of the samples. It is also found that the value of the lattice constant decreases with increases in La concentration. The magnetic properties of the samples were investigated by using a vibrating sample magnetometer (VSM). The results obtained from VSM show that the value of both magnetization (Ms) and coercivity (Hc) decreases with an increase in diamagnetic La concentration.

Keywords: Spinel ferrites, Sol-gel, SEM, TEM, VSM.

Introduction

The physical, electrical and magnetic properties of ferrites enable their use in various types of technologies. Spinel ferrite nanoparticle materials are highly preferred in engineering and technology applications, like biomedicine, pharmaceuticals, sensors, magnetic resonance imaging, drug delivery, microwaves, high-frequency devices, information storage and electronic chips [1, 2, 3, 4]. The structure and electromagnetic properties of nano-spinel ferrites can be modified by the substitution of different cations. Rare earth substitutions are highly valuable for reducing the particle size and intensification of the lattice parameter [5]. In this

respect, substituting rare earth (RE) cations into the spinel ferrite structure plays an important role in enhancing the dielectric, magnetic and electric properties due to the Fe-Fe interactions caused by the spin coupling effect of 3d electrons [6]. Therefore, when rare earth and iron interactions (3d-4f coupling) of the spinel ferrites occur, they can vary the structural, electrical, spectral and magnetic properties of spinel ferrites. In our study, structural changes, such as decreases in lattice constant due to the transfer of an equivalent number of Fe³⁺ ions (0.64 Å) from tetrahedral (A) site to octahedral [B] site to relax strain at the octahedral site, are observed. Magnetic parameters, such as

coercivity (H_c), saturation magnetization (M_s) and retentivity (M_r), decrease with an increase in La concentration. Different RE substitutions have proven to have different results on the ferrite structure [7,8,9]. Some researchers have investigated the effects of La substitution into cobalt-doped nickel ferrite [10-14].

Materials and Methods

Nano-sized ferrite particles with the composition $Ni_{0.2}Co_{0.8}Fe_{2-x}La_xO_4$ ($x = 0.02, 0.06, 0.10$) were prepared using sol-gel auto combustion method using urea as a fuel. The high-purity AR grade ferric nitrate ($Fe(NO_3)_3 \cdot 9H_2O$), Nickel nitrate ($Ni(NO_3)_2 \cdot 6H_2O$), Cobalt nitrate ($Co(NO_3)_2 \cdot 6H_2O$), Lanthanum nitrate ($La(NO_3)_3 \cdot 6H_2O$) are dissolved in distilled water. This solution was then heated at $80^\circ C$ for 4 to 5 hrs, to form sol to viscous brown gel. After that, it was kept in a microwave oven (Model IFB 17 PM – MEC1); within 2 to 3 min. auto combustion takes place and yields fine powder of $Ni_{0.2}Co_{0.8}Fe_{2-x}La_xO_4$ ferrite nanoparticles. The powder was sintered at $800^\circ C$ for 4 hrs.

Results and Discussion

X-ray Diffraction Analysis

The X-ray diffraction pattern for $Ni_{0.2}Co_{0.8}Fe_{2-x}La_xO_4$ ($x = 0.02, 0.06, 0.10$) synthesized by sol-gel auto combustion method is shown in Fig. 1. The XRD pattern confirmed the formation of single-phase cubic spinel with space group $Fd\bar{3}m$, which is in agreement with ICSD 174321. Measurements were performed using $Cu K\alpha$ radiation having a wavelength, $\lambda = 1.5406 \text{ \AA}$. Fig. 1 shows that the most intense diffraction peak (311) is slightly shifted towards a higher angle with increasing La substitution. The peak shift towards a higher angle can be attributed to a decrease in lattice parameter the reason behind which is that the lattice parameter is inversely proportional to the diffraction angle $\sin \theta$. When the diffracting angle (θ) increases, lattice constant (a) goes on decreasing.

The broadening of XRD peaks is related to the nano-sized particle and lattice strain. The value of lattice constant 'a' and particle size for each sample are given in (Table 1).

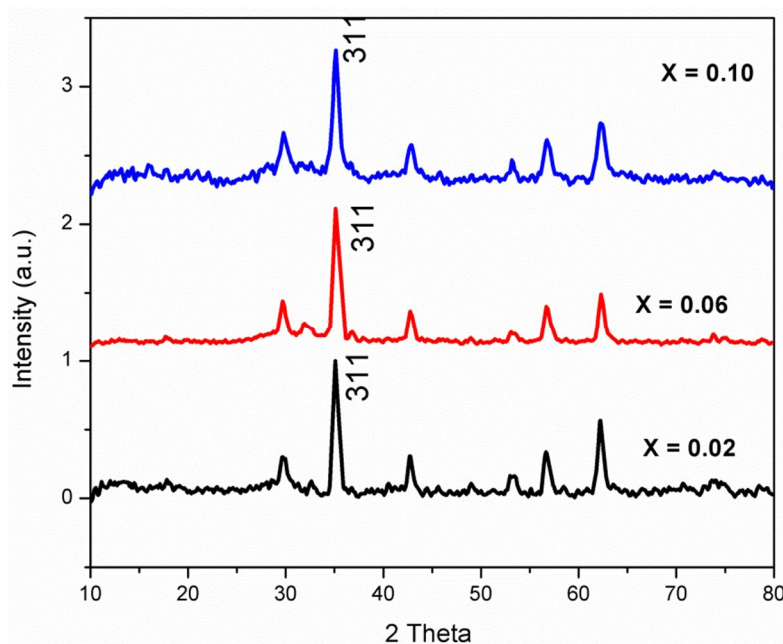


FIG. 1. XRD pattern of $Ni_{0.2}Co_{0.8}Fe_{2-x}La_xO_4$.

TABLE 1. Average particle size (D) and lattice constant (a).

Composition (X)	Average particle size (D) nm	Lattice constant (a) \AA
X = 0.02	10.34	8.48024
X = 0.06	11.89	8.47431
X = 0.10	8.56	8.46290

Note: Variation of average particle size (D) and lattice constant (a) of $Ni_{0.2}Co_{0.8}Fe_{2-x}La_xO_4$.

Morphological Analysis

The Field Emission Gun scanning electron microscopy (FEG-SEM) of Ni_{0.2}Co_{0.8}Fe_{2-x}La_xO₄ (x = 0.02, 0.06, 0.10) nanoparticles is shown in Fig 2. The image exhibits a higher agglomeration cubic shape with an average grain size of 39 nm. The existence of agglomeration may be due to the interaction between the magnetic particles [12].

The EDX spectrum confirmed the existence of Ni, Co, Fe, La and O in composition X = 0.02, 0.06 and 0.10, as shown in Fig 3. The EDX spectra illustrate that La peak intensities increase with an increase in La content. The TEM pattern of Ni_{0.2}Co_{0.8}Fe_{2-x}La_xO₄ (x = 0.02) nanoparticles is shown in Fig. 4. The image confirms the cubic spinel structure. Fig 5 shows the Selected Area Electron Diffraction (SAED) image which also confirms the formation of poly-nanocrystalline form.

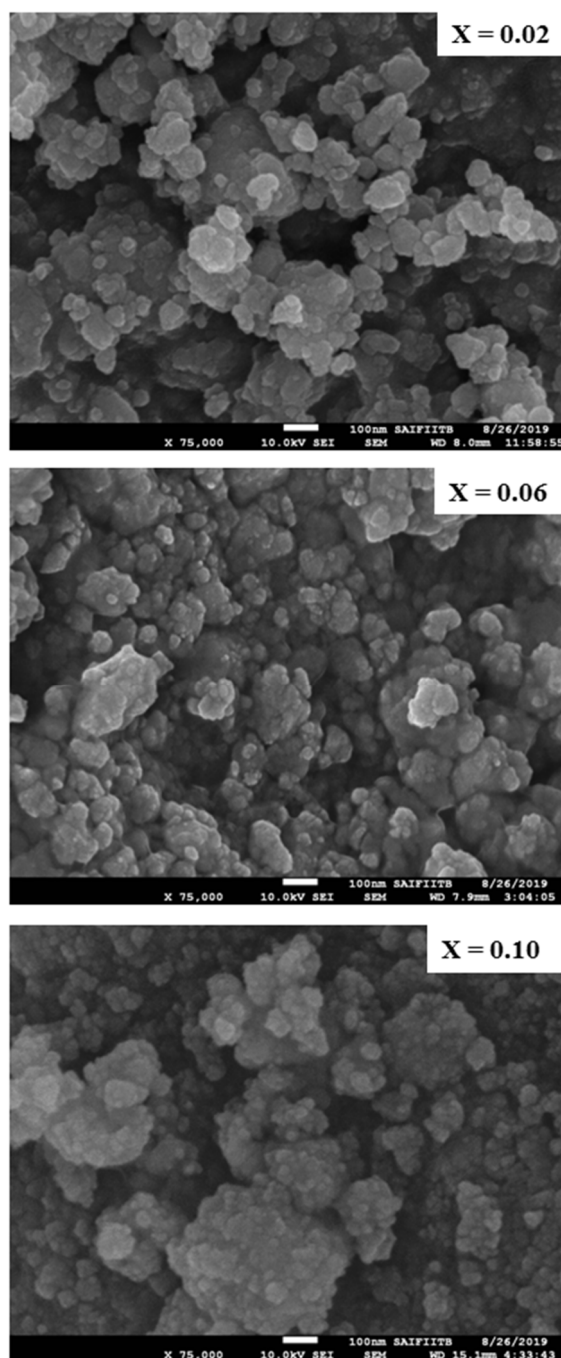


FIG 2. Field emission gun scanning electron microscopy (FEG- SEM) of Ni_{0.2}Co_{0.8}Fe_{2-x}La_xO₄ for different concentrations of X.

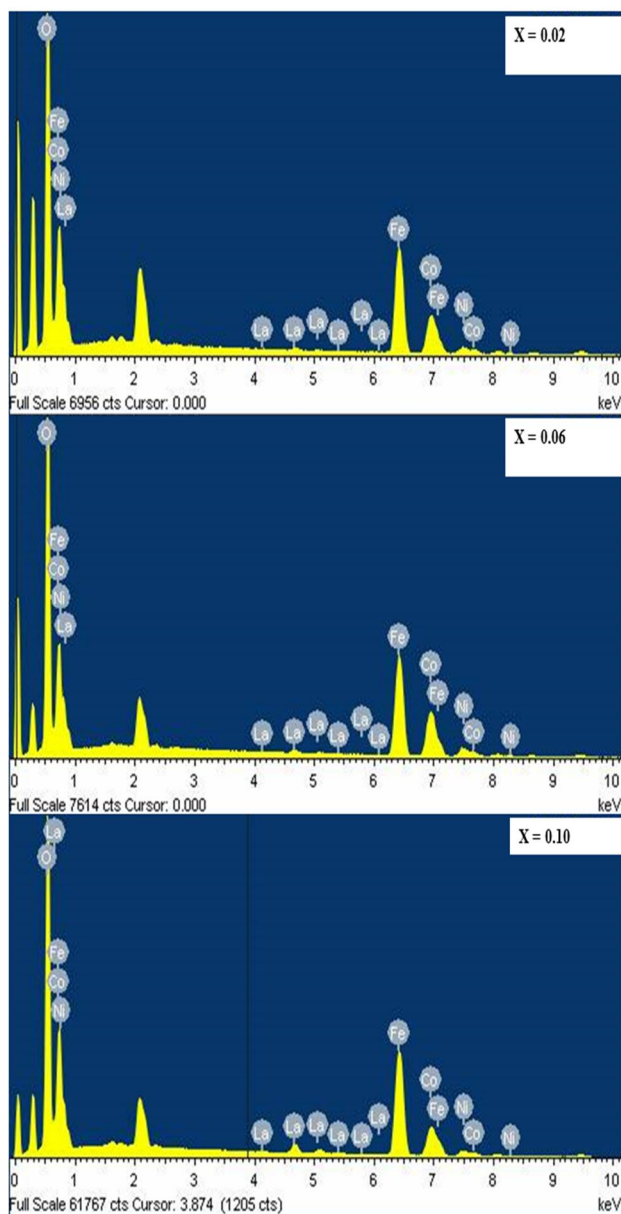


FIG. 3. EDX of $\text{Ni}_{0.2}\text{Co}_{0.8}\text{Fe}_{2-x}\text{La}_x\text{O}_4$ for different concentrations of x .

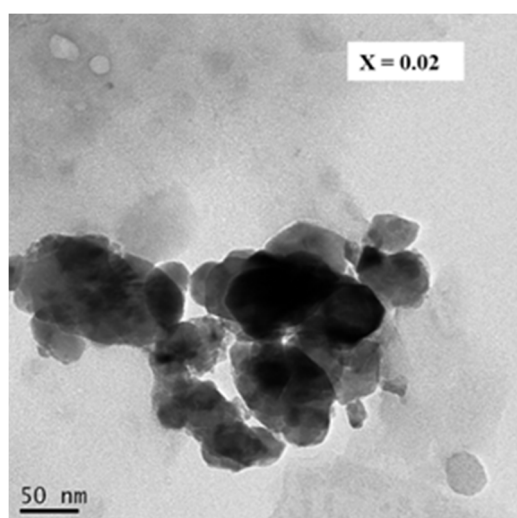


FIG. 4. The field emission gun transmission electron microscopy (FEG-TEM) of $\text{Ni}_{0.2}\text{Co}_{0.8}\text{Fe}_{2-x}\text{La}_x\text{O}_4$ for ($x = 0.02$).

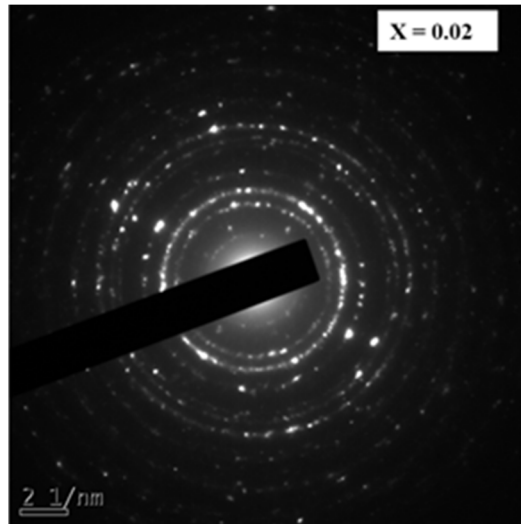


FIG. 5. The SAED image of Ni_{0.2}Co_{0.8}Fe_{2-x}La_xO₄ for (X = 0.02).

Magnetic Properties

At room temperature, magnetization as a function of the applied magnetic field is shown in Fig. 6 for different samples. All samples show a typical magnetic characteristic of ferrites with a difference in the value of saturation magnetization (Ms). The saturation magnetization value (Ms) and coercivity (Hc) have been found to decrease with the increase in La concentration. In the rare-earth substituted ferrites, the rare-earth ions have a strong preference for the octahedral lattice site (B) of the spinel lattice. Neel has explained the magnetic behavior of these spinels based on the

exchange interaction that occurs between metal ions at A & B sites spinel. Fig. 7a and Fig. 7b show tetrahedral A sites and octahedral B sites, respectively. [15-18]. It was expected that a fraction of La ion enters into octahedral sites and creates distortions as well as a decrease in lattice constant. This is in agreement with the findings in this work (Table 1). Thus, the observable decreases in coercivity (Hc) and saturation magnetization (Ms) may be attributed to the larger lattice distortion and smaller crystalline size. The values of saturation magnetization (Ms), coercivity (Hc) and retentivity (Mr) for all three samples are tabulated in (Table 2).

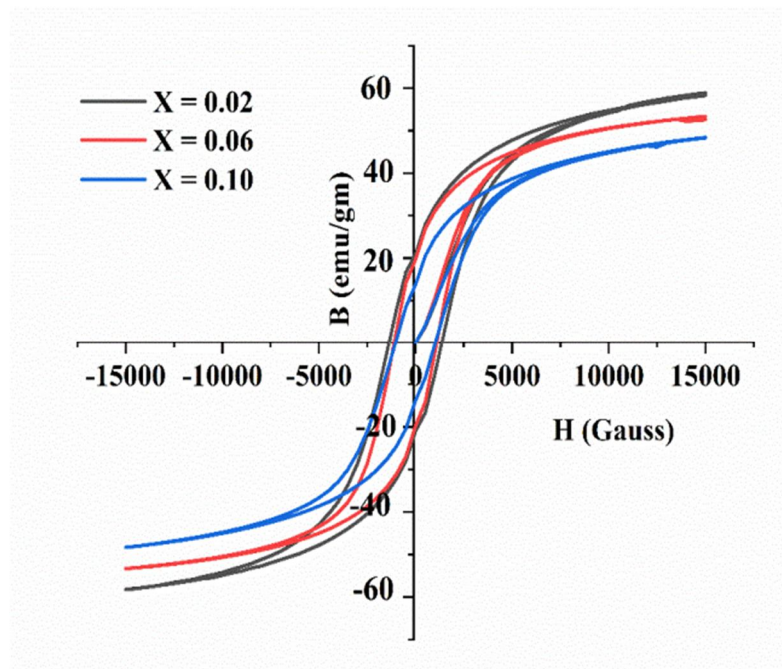


FIG. 6. Hysteresis loop for Ni_{0.2}Co_{0.8}Fe_{2-x}La_xO₄.

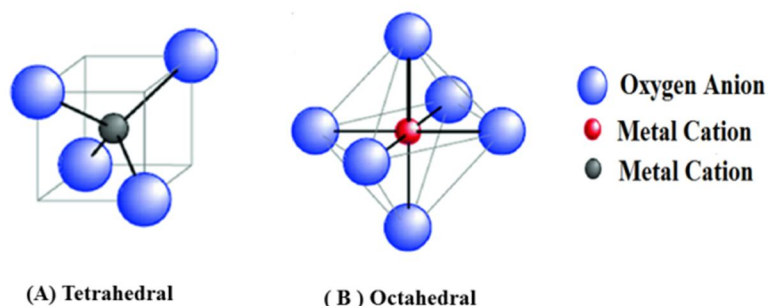


FIG. 7. (a) Tetrahedral (A) sites and (b) Octahedral (B) sites.

TABLE 2. Values of coercivity (H_C), retentivity (Mr) and saturation magnetization (Ms) for $Ni_{0.2}Co_{0.8}Fe_{2-x}La_xO_4$.

Composition (X)	H_C (G)	Mr (emu/gm)	Ms (emu/gm)
X = 0.02	1366.2	20.92	58.58
X = 0.06	1105.0	19.67	53.34
X = 0.10	1031.6	13.75	48.36

Conclusion

In this work, a series of $Ni_{0.2}Co_{0.8}Fe_{2-x}La_xO_4$ ($X = 0.02, 0.06$ and 0.10) powders and sintered samples were successively prepared by sol-gel auto combustion method using oxide as precursor and urea as fuel. The structural properties were investigated by XRD. XRD confirmed the formation of the FCC spinel phase for all the samples. The EDX spectrum shows that no additional impurity is present in the sample. It also shows that the lattice constant 'a' decreases with the increase in La concentration.

The particle size calculated from X-ray diffraction is approximately constant. The SAED image also confirms the formation of a polynanocrystalline sample. Further, La-substituted $NiCoFe_2O_4$ ferrite shows a definite hysteresis loop at room temperature. The presence of non-magnetic La in $NiCoFe_2O_4$ ferrite results in a reduction of coercivity (H_c), saturation magnetization (Ms) and retentivity (Mr), which could be due to dilution in the magnetic interaction.

References

- [1] Chen, Q. and Zhang, Z.J., *Appl. Phys. Lett.*, 73 (1998) 3156.
- [2] Zhao, L., Yang, H., Yu, L., Cui, Y., Zhao, X. and Feng, S.J., *Mater. Sci.*, 42 (2007) 686.
- [3] Kumar, E.R., Kamzin, A.S. and Janani, K.J., *J. Magn. Magn. Mater.*, 417 (2016) 122.
- [4] Kumar, E.R., Jayaprakash, R. and Patel, R., *Superlattices and Microstructures*, 62 (2013) 277.
- [5] Das Calu, G., Popescu, T., Feder, M. and Caltun, O.F., *J. Magn. Magn. Mater.*, 333 (2013) 69.
- [6] Shah, M.S., Ali, K., Ali, I., Mahmood, A., Ramay, S.M. and Farid, M.T., *Mater. Res. Bull.*, 98 (2018) 77.
- [7] Junaid, M., Khan, M.A., Iqbal, F., Murtaza, G., Akhtar, M.N., Ahmad, M., Shakir, I. and Warsi, M.F., *J. Magn. Magn. Mater.*, 419 (2016) 338.
- [8] Boda, N., Boda, G., Naidu, K.C.B., Srinivas, M., Batoo, K.M., Ravinder, D. and Reddy, A.P., *J. Magn. Magn. Mater.*, 473 (2019) 228.
- [9] Kokare, M.K., Jadhav, N.A., Singh, V. and Rathod, S.M., *Opt. Laser Technol.*, 112 (2019) 107.
- [10] Kumar, P., Sharma, S.K., Knobel, M., Chand, J. and Singh, M., *J. Electroceram.*, 27 (2011) 51.
- [11] Mansour, S.F., Hemedat, O.M., El-Dek, S.I. and Salem, B.I., *J. Magn. Magn. Mater.*, 420 (2016) 7.

- [12] Vadivel, M, Ramesh Babu, R., Arivanandhan, M. and Ramamurthi, K., *Journal of Superconductivity and Novel Magnetism*, 30 (2017) 441.
- [13] Yadav, R.S., Kuritka, I., Vilcakova, J., Havlica, J., Kalina, L., Urbánek, P., Machovsky, M., Masar, M. and Holek, M., *Journal of Materials Science: Materials in Electronics*, 28 (2017) 9139.
- [14] Kumar, L. and Kar, M., *Ceram. Inter.*, 38 (2012) 4771.
- [15] Karimi, Z., Mohammadifar, Y., Shokrollahi, H., Asl, S.K., Yousefi, G. and Karimi, L., *J. Magn. Magn. Mater.*, 361 (2014) 150.
- [16] Ghone, D.M., Mathe, V.L., Patankar, K.K. and Kaushik, S.D., *J. Alloys Compd.*, 739 (2018) 52.
- [17] Wu, X., Ding, Z., Song, N., Li, L. and Wang, W., *Ceram. Int.*, 42 (2016) 4246.
- [18] Neel, L., *Ann. Phy.*, 3 (1948) 137.